UC Davis
UC Davis Previously Published Works

Title

Oximetry with the NMR signals of hemoglobin Val E11 and Tyr C7

Permalink

https://escholarship.org/uc/item/0bx2281g

Journal

European Journal of Applied Physiology, 107(3)

ISSN

1439-6327

Authors

Xie, Hongtao

Kreutzer, Ulrike

Jue, Thomas

Publication Date

2009-10-01

DOI

10.1007/s00421-009-1125-3

Peer reviewed

ORIGINAL ARTICLE

Oximetry with the NMR signals of hemoglobin Val E11 and Tyr C7

Hongtao Xie · Ulrike Kreutzer · Thomas Jue

Abstract The NMR visibility of the signals from erythrocyte hemoglobin (Hb) presents an opportunity to assess the vascular PO_2 (partial pressure of oxygen) in vivo to gather insight into the regulation of O_2 transport, especially in contracting muscle tissue. Some concerns, however, have arisen about the validity of using the Val E11 signal as an indicator of PO_2, since its intensity depends on tertiary structural changes, in contrast to the quaternary structure changes associated with relaxed (R) and tense (T) transition during O_2 binding. We have examined the Val E11 and Tyr C7 signal intensity as a function of Hb saturation by developing an oximetry system, which permits the comparative analysis of the NMR and spectrophotometric measurements. The spectrophotometric assay defines the Hb saturation level at a given PO_2 and yields standard oxygen-binding curves. Under defined PO_2 and Hb saturation values, the NMR measurements have determined that the Val E11 signal, as well as the Tyr C7 signal, tracks closely Hb saturation and can therefore serve as a vascular oxygen biomarker.

Keywords Muscle · Oxygen transport · Oxygen · Myoglobin · Bioenergetics

Introduction

The detection of the ^1H NMR Mb (myoglobin) signals in vivo has presented an approach to measure intracellular oxygenation under different physiological conditions

H. Xie · U. Kreutzer · T. Jue (✉)
Department of Biochemistry and Molecular Medicine,
University of California Davis, Davis, CA 95616-8635, USA
e-mail: TJue@ucdavis.edu

(Chung et al. 2005; Ponganis et al. 2008; Kreutzer et al. 1992). Such measurements provide insight into the role of O_2 in regulating bioenergetics, especially during muscle contraction. Because these signals also appear in Hb, an opportunity exists to assess both the vascular and intracellular PO_2 to clarify the regulatory interaction between metabolism and oxygen transport (Kreutzer et al. 1993; Fetler et al. 1995).

In particular, the NMR methodology depends on the protein structural transition during oxygenation and deoxygenation, which alters the intensity of the proximal histidyl $N_\delta H$ and $\gamma CH_3 Val$ E11 signals. Given the normalized signal intensity and the in vitro O_2 association constant, experiments can determine the intracellular PO_2 (Jue 1994; Kreutzer et al. 1992). For the proximal histidyl $N_\delta H$, its signal intensity reaches a maximum in the fully deoxygenated state. Using the Val E11 avoids the anoxia condition, because the signal reaches a maximum intensity in the oxygenated state. Moreover, using the ratio of the proximal histidyl $N_\delta H$ and $\gamma CH_3 Val$ E11 signals helps discriminate signal intensity changes arising from oxygenation instead of blood volume (Kreutzer et al. 1992).

However, unlike monomeric Mb, the Val E11 signal intensity of tetrameric Hb reflects both tertiary and quaternary structural changes. Some researchers have raised concerns that the Val E11 signal intensity might not report accurately the state of Hb saturation (Fetler et al. 1995). The concern predicates on the Perutz's interpretation of the Monod, Wyman and Changeux (MWC) two-state model of Hb oxygen binding. Only the movement of the proximal histidine links directly to the hydrogen bonding at the subunit interface as the quaternary structure shifts between the relaxed (R) to tense (T) state (Monod et al. 1965; Weissbluth 1974; Perutz 1989; Perutz et al. 1998; Bruno et al. 2001). The model does not associate specifically a T

to R transition with any structural perturbation affecting the Val E11.

We have hypothesized that the R to T quaternary structural change affects similarly the signals of γCH_3 Val E11 and Tyr C7, a quaternary state marker at the subunit interface. These signals will reflect accurately the state of Hb oxygenation. We have conducted a comparative spectrophotometric and NMR study of Hb with and without inositol hexaphosphate (IHP), a stable analog of the endogenous BPG (2, 3 bisphophoglycerate) allosteric effector found in erythrocytes, and at different values of pH and PO_2. Indeed, the spectrophotometric and NMR assays yield oxygen-binding curves in excellent agreement with previous literature reports (Chang et al. 2002; Gong et al. 2006; Lukin and Ho 2004; Asakura and Lau 1978; Benesch et al. 1967; Rossi-Fanelli et al. 1961). As a consequence, the results confirm that ^{1}H NMR signal of either the γCH_3Val E11 or Tyr C7 responds sensitively to the structural changes in the R to T transition, reports accurately the Hb oxygenation state, and can serve as a vascular oxygen biomarker.

Materials and methods

In vitro experiment preparation

Hemoglobin was prepared as previously reported (Kreutzer et al. 1993; Wang et al. 1997). Fresh outdated red blood cells were centrifuged for 15 min at $600 \times g$ and washed three times with 1% NaCl solution. For Hb solution experiments, the erythrocytes were lysed with three volumes of distilled H_2O and contaminant proteins precipitated with 20% of saturated ammonium sulfate. The lysate was centrifuged for 30 min at $10,000 \times g$ and then dialyzed against 100 mM potassium phosphate buffer (pH 7.4). Bubbling CO then converted the HbO_2 to HbCO, which was stored at 4°C. Converting HbCO to HbO_2 required a bright light to photodissociate CO from cold HbCO under a stream of O_2.

All Hb samples used for optical and NMR studies were 0.025 or 0.125 mM in Hb tetramer in 100 mM phosphate buffer at pH 7.0. Concentration of HbO_2 and deoxy Hb on a heme basis was determined by spectrophotometric measurement (UVIKON 941, Kontron Instruments) of the Hb bands. Extinction coefficients of $\varepsilon_{541} = 13.8$ mM^{-1} cm^{-1}, $\varepsilon_{577} = 14.6$ mM^{-1} cm^{-1} and $\varepsilon_{555} = 12.5$ mM^{-1} cm^{-1} (Antonini and Brunori 1971) were used to calculate Hb concentration. Visible spectra of the Hb samples were taken before and after the NMR experiment to measure HbO_2 concentration and to detect the presence of any metHb. Only data from samples with no detectable metHb were used in the analysis.

Oxygen equilibration system

Appropriate HbO_2 saturations were obtained by equilibrating Hb solution in a home-built system shown in Fig. 1. The closed loop system consists of a peristaltic pump (Cole-Parmer, Cartridge pump model: 07519-15), tubing (Pharmed, Lot No.: 201923), gas-mixing chamber with O_2 permeable silastic tubing (Dow Corning, Cat.No.: 508-006), polarographic oxygen monitor (Cameron Instruments, OM2000), gas mixer (Cameron Instruments, GF-4/MP) and humidifier. The pump circulated about 40 ml of humidified HbO_2 through the silastic tubing wrapped around a plastic rack, which maximized the surface area for O_2 exchange, and then through an NMR tube and/or cuvette. At a flow rate of 40 ml/min, the entire solution volume passed through the system within 1 min. The gas mixer introduced a precise ratio of O_2 or N_2 into the gas-mixing chamber to achieve different PO_2. An oxygen meter equipped with a Clark-type oxygen electrode determined the PO_2 of the HbO_2 solution. A spectrophotometer then measured the HbO_2 signals from 450 to 650 nm with 1 nm resolution. The NMR spectrometer recorded the ^{1}H NMR signals of Hb in the presence or absence of IHP and at identical PO_2 values. A 5 μm
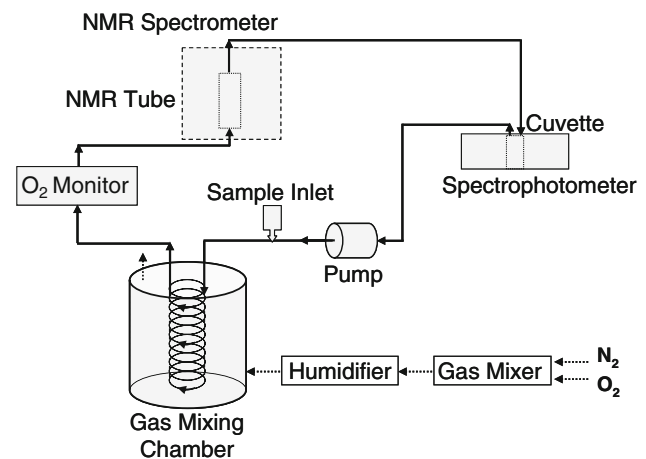

Fig. 1 The oxygen equilibration system that permits coordinated spectrophotometric and NMR measurements: The system components comprise a peristaltic pump, gas-mixing chamber with O_2 permeable tubing, a gas mixer to create different mixtures of O_2 and N_2, an O_2 monitor, spectrophotometer or NMR spectrometer, and connecting tubings to form a closed loop. Hb injected into inlet port circulates into the gas-mixing chamber, where it equilibrates with the O_2/N_2 mixture defined by the gas mixer. The equilibrated Hb solution loops through either a spectrophotometer switch or an NMR spectrometer switch. For spectrophotometric assay, the Hb solution would circulate through a cuvette as the spectrophotometer records the optical spectra. For the NMR assay, the Hb solution would enter the NMR tube from the bottom and recirculate into the gas-mixing chamber. The NMR spectrometer would record the ^{1}H NMR spectra. A typical experiment utilizes 40 ml of Hb, which circulates at 40 ml/min

Millipore (Millipore, Molsheim) filter removed any particulate material.

Oxygen-binding curve

A spectrophotometer determined the O_2-binding curves of 0.025 mM Hb in 100 mM inorganic phosphate (Pi) buffer as a function of pH (6.6–7.5) with and without IHP at 25°C. Sodium inositol hexaphosphate (IHP) was added in IHP:Hb (tetramer) molar ratio of 5:1. The addition of 0.1 N HCl or 0.1 N NaOH adjusted the pH of HbO_2 as verified by a Corning (Model 240) pH meter. The spectrophotometer recorded the Hb saturation after a cycle of deoxygenation and reoxygenation at 0, 1, 1.5, 2, 3, 5, 7, 10 and 21% O_2, corresponding to PO_2 values between 0 and 154 mmHg. Each PO_2 step required about 7 min to equilibrate with the different PO_2. Two spectra were recorded for each PO_2 step. A complete experiment usually required about 90 min. After the experiment, sodium dithionite was added to create the totally desaturated Hb state and the associated reference spectrum.

HbO$_2$ fractional saturation

The fractional HbO_2 saturation $Y = \frac{HbO_2}{HbO_2 + Hb}$ was determined from the absorbance change in the HbO_2 β (541 nm) and α (577 nm) and the deoxy Hb (555 nm) bands. The analysis of the curve fit of Y versus PO_2 with either the equation

$$Y = \frac{PO_2^{n_{Hill}}}{PO_2^{n_{Hill}} + P_{50}^{n_{Hill}}} \tag{1}$$

or with the Hill equation

$$\log \frac{Y}{1-Y} = n_{Hill} \log PO_2 \tag{2}$$

led to the determination of the P_{50} (partial O_2 pressure at 50% saturation) and the Hill coefficient, n_{Hill}.

NMR

^{1}H NMR experiments were performed on an Avance 400-MHz Bruker NMR spectrometer using a 20-mm microimaging probe (R31/1 20-40/MI-400-R014). A specially designed sample NMR tube was mounted inside the probe with the entrance port at the bottom and the exit port at the top. After equilibrating the Hb to a specified PO_2, the Hb flowed into the probe from the bottom of the magnet and exited from the top to form a closed loop system. Typical experiment used 0.125 mM HbA in 100 mM Pi buffer at 25°C. Chemical shifts were referenced to the water proton signal at 4.75 ppm 25°C, calibrated against 2-dimethyl-2-silapentane-5-sulfonate (DSS).

The ^{1}H NMR signals were normalized to Hb signals under fully oxygenated or deoxygenated conditions. After the NMR experiment, the relative signal intensities (integrated peak areas) of ^{1}H NMR peaks at each oxygenation state were determined by normalizing the signal intensity to its full oxygenated and deoxygenated condition.

A 1–5–10–10–5–1 pulse sequence suppressed the water signal and produced a sufficient uniform excitation profile in the region of interest (Hore 1983). A typical HbO_2 spectrum used 8 kHz spectral width, 1 K data points and 512 scans. The 90° pulse calibrated against the water proton signal was 50 μs. Zero-filling improved the spectral resolution. Apodizing the free induction decay (FID) with an exponential or an exponential-Gaussian window function improved the spectra. A spline fit then smoothed the baseline.

Statistical analysis

Statistical analysis used the Sigma Plot/Sigma Stat program (Systat Software, Inc., Point Richmond, CA) and expressed the values as mean value ± standard deviation (SD). Statistical significance was determined by two-tailed unequal variance Student's t test with no statistical difference indicated by $P > 0.05$.

Results

Figure 1 shows the schematic representation of the closed loop system, which contains Hb circulating through a gas-mixing chamber, O_2 monitor and an NMR tube or a spectrophotometer cuvette. A gas mixer supplies a specific mixture of N_2 and O_2 to the chamber, which allows the Hb solution to equilibrate at a defined PO_2. A spectrophotometer monitors the changes in the Hb bands to ensure full equilibration. After the Hb has equilibrated, these bands lead to the determination of the Hb saturation. A plot of the Hb saturation as a function of PO_2 yields the oxygen-binding curve. With the identical protocol, NMR can correlate the changes in the Val E11 and Tyr C7 signals, a tertiary and quaternary protein structure marker, respectively (Acharya et al. 2003; Chang et al. 2002; Dalvitt and Ho 1985; Gong et al. 2006; Lukin and Ho 2004; Viggiano et al. 1979). Table 1 tabulates the P_{50} and n_{Hill} of Hb at different pH values as determined by optical and NMR methods.

Figure 2 shows the visible spectra of 0.025 mM HbO_2 in 100 mM Pi buffer pH 7.0 at 25°C with IHP (Fig. 2a) and without IHP (Fig. 2b) at PO_2 between 2.6 and 155 mmHg. Keeping the temperature at 25°C ensures protein stability during the course of the experiment. The β and α bands at 541 and 577 nm fall as the PO_2 decreases (Fig. 2a). In contrast, the deoxy Hb signal at 555 nm rises. Without IHP, Hb shows a sharper change in oxygen saturation

Table 1 Optical and NMR determined O$_2$-binding parameters for Hb A

pH	IHP		No IHP	
	P_{50} (mmHg)	n_{Hill}	P_{50} (mmHg)	n_{Hill}
Optical				
6.6	51.28	2.29	17.05	2.85
6.8	45.43	2.18	15.73	2.93
7.0	40.75	2.27	13.20	2.73
7.2	31.06	2.52	10.98	2.90
7.3	26.44	2.73		
7.5	21.75	2.77		
NMR				
7.0				
Val E11 (−2.48 ppm)	55.72	2.02	12.94	2.62
Tyr C7 (14.0 ppm)	45.12	1.52	11.87	3.44

Fig. 2 A representative set of optical spectra of 0.025 mM HbO$_2$ in 100 mM Pi buffer at pH = 7.0 at 25°C **a** with IHP **b** without IHP. The oxygen equilibration system presents a defined O$_2$ mixture to establish different Hb saturation states. The resultant Hb spectra show the changes in the β (577 nm) and α (541 nm) of HbO$_2$, as well as the 555 nm band of deoxy Hb. Partially oxygenated samples were obtained by equilibrating Hb in a mixture of O$_2$ and N$_2$, starting from 0, 1, 2, 3, 5, 7, 10 to 21% O$_2$, corresponding to PO$_2$ between 0 and 154 mmHg. Each oxygen saturation step requires about 7 min to reach a steady state. In the IHP experiments, IHP exists in a 5:1 molar ratio of IHP:Hb

(Fig. 2b). Table 2 shows the P_{50} and Hill coefficient of Hb at different pH values and with or without the allosteric effector, IHP.

The analysis of the visible spectra yields the Hb saturation (Y) as a function of PO$_2$. Figure 3a plots Y against PO$_2$ to produce the O$_2$-binding curves for Hb in the presence of IHP from pH 6.6 to 7.5. The corresponding O$_2$-binding curves in the absence of IHP show a pronounced left shift, reflecting a higher O$_2$ affinity (Fig. 3b).

Given the O$_2$-binding curve, the analysis based on Eqs. 1 and 2 yields the pH-dependent P_{50} and n_{Hill} of Hb with and without IHP over the pH range from 6.6 to 7.5 (Fig. 4). The values of these Hb parameters stand in excellent agreement with previous literature reports (Tables 1, 2; Chang et al. 2002; Gong et al. 2006; Lukin and Ho 2004).

Figure 5 shows the ^{1}H NMR spectra of the Tyr C7 peak at 14.0 and the Val E11 peak at −2.48 ppm in the presence (left panel) and absence (right panel) of IHP at PO$_2$ values from 2.8 mmHg. The proton shared in the H-bond between α_1 Tyr C7 and β_2 Asp 99 in the T state gives rise to 14 ppm signal and reflects the quaternary structural change at the subunit interface during R to T transition (Ho and Russu 1981). As the quaternary state shifts from T to R with increasing PO$_2$, the Tyr C7 signal intensity decreases. The Val E11 signal of HbO$_2$ at −2.48 serves as a marker of Hb tertiary structure in the heme pocket. In contrast, its intensity rises as Hb saturation increases (Acharya et al. 2003; Chang et al. 2002; Dalvitt and Ho 1985; Gong et al. 2006; Lukin and Ho 2004; Viggiano et al. 1979).

Figure 6 overlays the measured Hb saturation at pH 7.4 and 25°C, as determined by spectrophotometry and NMR. With and without IHP, the tertiary and quaternary structural markers, as reflected in the Val E11 and Tyr C7 signals, track closely the changes in Hb saturation. Table 3
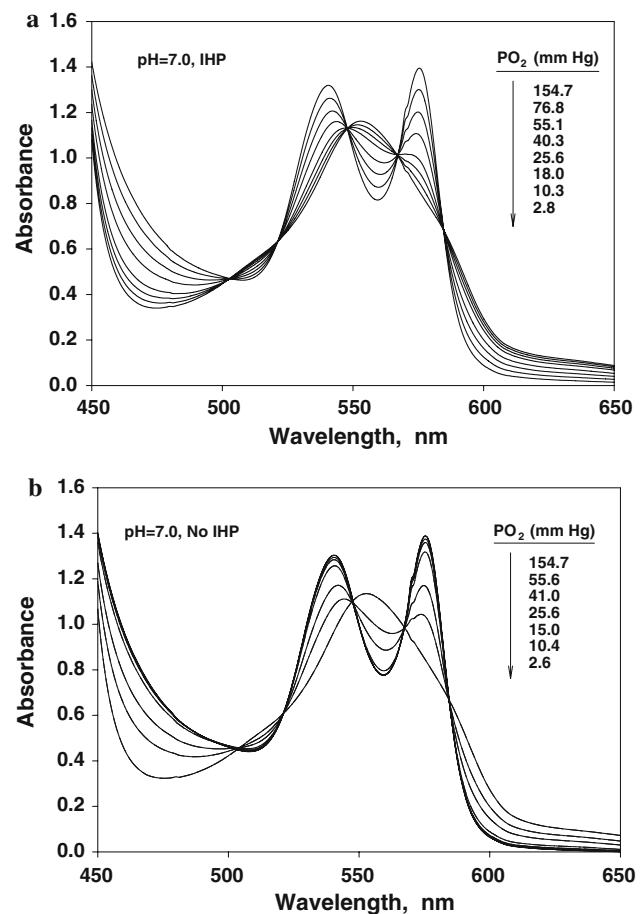
summarizes the comparison between the spectrophotometric and NMR results. At each oxygen steady state, PO$_2$, with and without IHP, HbO$_2$ saturation determined by optical ($n = 3$) and by NMR measurements ($n = 4$–7) shows no statistical significant difference ($P > 0.05$).
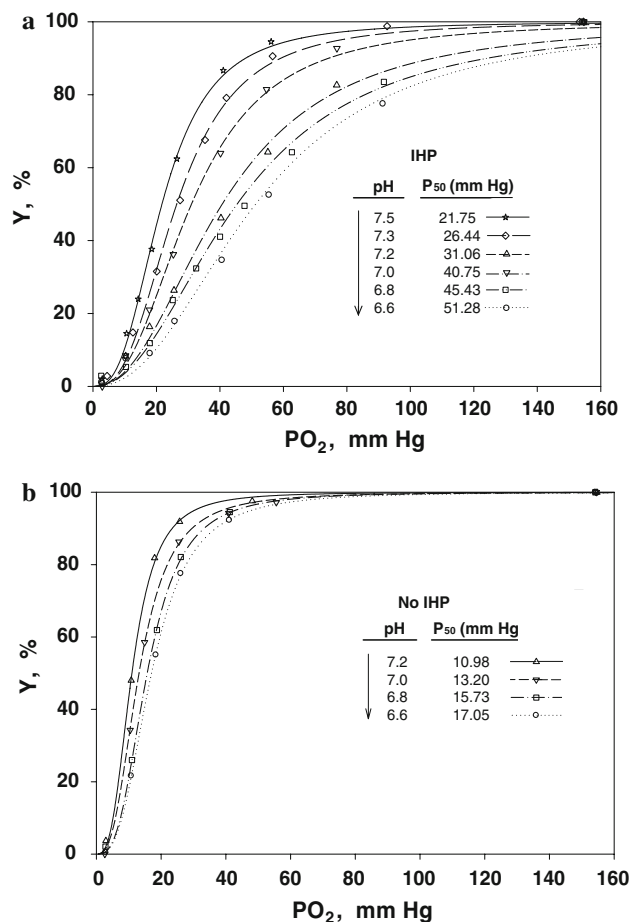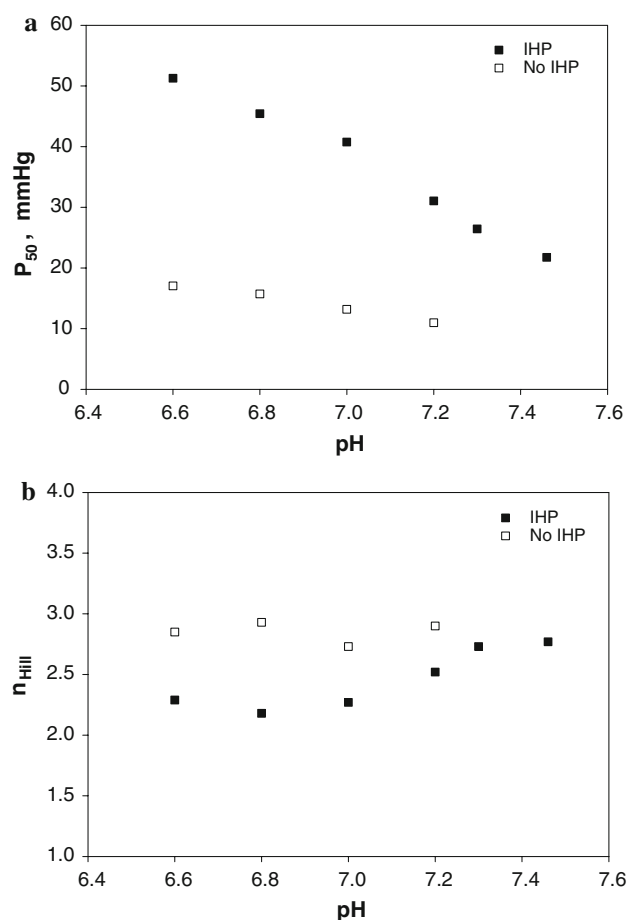
Discussion

Hb oximetry

The closed loop oxygen equilibration system overcomes a major hurdle in studying the structure and function of Hb by establishing a methodological approach to determine the

Table 2 Comparative analysis of O_2-binding parameters for Hb A

[IHP]/[Hb]	pH	Temp °C	P_{50} mmHg	n_{Hill}	References
0	6.98	29	14.57	2.9	Lukin and Ho (2004)
0	7.08	29	15.90	3.2	Chang et al. (2002)
0	7.00	20	8.70	2.7	Asakura and Lau (1978)
0	7.00	20	12.02	2.9	Rossi-Fanelli et al. (1961)
0	7.00	25	13.20	2.7	This work
0	7.22	29	13.90	3.2	Chang et al. (2002)
0	7.20	25	10.98	2.9	This work
3	7.00	35	40.00	2.4	Gong et al. (2006)
50	7.00	15	37.80	2.1	Benesch et al. (1967)
5	7.00	25	40.75	2.3	This work
50	7.40	15	22.20	2.6	Benesch et al. (1967)
5	7.50	25	21.75	2.8	This work

[Hb] is 0.025 mM

Fig. 4 Plot of P_{50} and n_{Hill} of Hb A as a function of pH at 25°C with IHP and without IHP. **a** In the presence of IHP, P_{50} decreases from 51.28 to 21.75 as pH increases from 6.6 to 7.5. Without IHP, P_{50} decreases only from 17.05 to 10.98, as pH increases from 6.6 to 7.2. **b** HbO$_2$ with IHP shows n_{Hill} increasing from 2.29 to 2.77 as pH increases from 6.6 to 7.5. Without IHP, the n_{Hill} changes from 2.85 to 2.90 as pH rises from 6.6 to 7.2

Fig. 3 Oxygen-binding curves of HbO$_2$ at different pH values in 100 mM Pi buffer at 25°C **a** with IHP **b** without IHP. IHP right shifts the P_{50} at pH 7.0 from 13.20 to 40.75. Y is percentage of HbO$_2$. *Error bars* representing standard deviation are too small to detect in the figure

spectral characteristics, given a defined Hb saturation at a specified PO_2, pH, allosteric modulation and temperature for both spectrophotometric and NMR experiments. The system avoids the experimental uncertainty of defining Hb saturation by mixing HbO$_2$ with deoxy Hb (Fetler et al. 1995; Viggiano and Ho 1979). Such a mixing protocol does not always define the state of Hb saturation, because it assumes that the Hb saturation will reflect the fractional amount of HbO$_2$ in the mixture. It does not account for the contribution from any dissolved O_2 in the solution or from the action of any residual dithionite used to remove excess O_2 in the deoxy Hb solution.

With the oxygen equilibration system, the spectrophotometric assay shows that the β (541 nm) and α (577 nm) bands of HbO$_2$ decline with decreasing PO_2. Conversely, the deoxy Hb signal at 555 nm increases. At present, the oximeter system can reach a PO_2 of about 3 mmHg. No
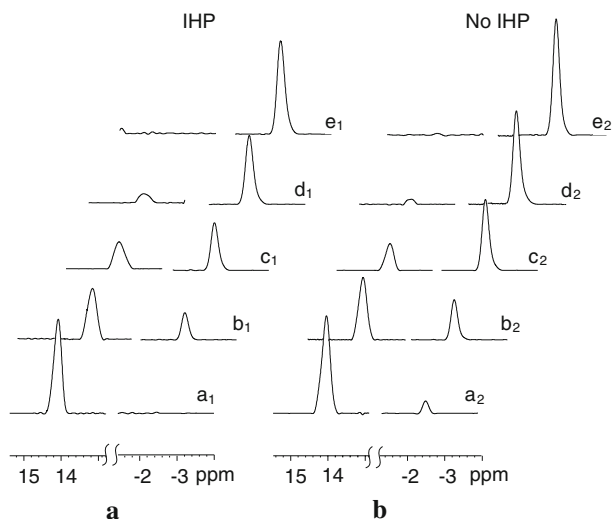
Fig. 5 ^{1}H NMR spectra of Val E11 and Tyr C7 as a function of Hb oxygenation **a** with IHP **b** without IHP. As PO_2 increases, the Tyr C7 signal at 14.0 ppm falls, while the Val E11 signal at −2.48 ppm rises. The spectra show HbO$_2$ at 0, 12.5, 25, 50, 75 and 100% oxygenation
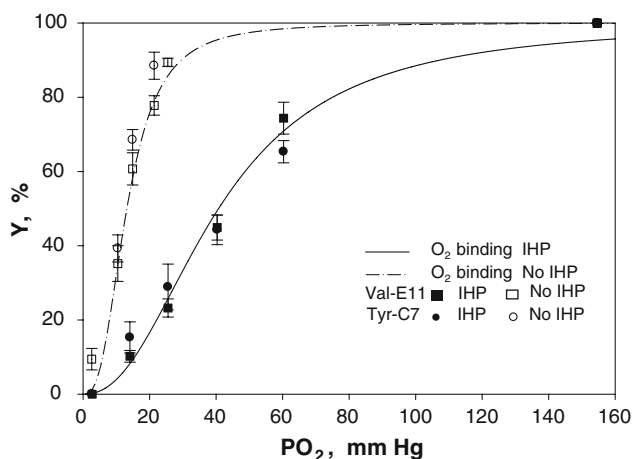

Fig. 6 Plot of Hb saturation versus PO_2 as determined by spectrophotometry and by the NMR signals of Val E11 and Tyr C7. The *solid* and *dashed lines* show the oxygen-binding curves of HbO$_2$ with and without IHP. Overlaying these lines are the corresponding changes in the NMR signals of the Val E11 (*filled square*) and the Tyr C7 (*filled circle*) of Hb in the presence of IHP, and the Val E11 (*open square*) and the Tyr C7 (*open circle*) signals of Hb in the absence of IHP. *Error bars* represent standard deviation

significant Hb degradation to metHb appears during the course of the spectrophotometry experiments. The plot of Hb saturation as a function of PO_2 yields the familiar oxygen-binding curves:

At 25°C and without IHP, Hb at pH 7.2 exhibits a P_{50} of 10.98 mmHg and a n_{Hill} of 2.90. With IHP and Hb at a ratio of 5:1, the O$_2$-binding curve right shifts as the Hb decreases its O$_2$ affinity. Hb P_{50} increases to 31.06 mmHg, while n_{Hill} decreases to 2.52. As pH decreases from pH 7.2 to 6.6 in the absence of IHP, the P_{50} also increases from

Table 3 HbO$_2$ saturation determined by spectrophotometry and NMR

PO_2 (mmHg)	$Y_{Optical}$ (%)	Y_{Tyr-C7} (%)	Δ_1 (%)	$Y_{Val-E11}$ (%)	Δ_2 (%)
With IHP					
2.8	1.4 ± 1.0	0.0	1.4	0.0	1.4
14.1	12.2 ± 3.7	15.3 ± 3.9	3.1	10.2 ± 1.9	2.0
25.6	26.3 ± 5.1	28.9 ± 5.7	2.6	23.2 ± 3.0	3.1
40.3	46.2 ± 3.7	44.3 ± 2.0	1.9	44.9 ± 4.1	1.3
60.3	68.7 ± 1.9	65.3 ± 2.7	3.4	74.3 ± 6.3	5.6
154.5	100.0 ± 0.8	100.0	0.0	100.0	0.0
Without IHP					
2.6	2.7 ± 1.5	100.0	2.7	9.4 ± 2.9	6.7
10.4	34.3 ± 1.1	39.3 ± 3.6	5	35.0 ± 4.8	0.7
14.9	58.5 ± 4.6	68.5 ± 2.8	10	60.7 ± 4.3	2.2
21.4	79.0 ± 5.4	88.5 ± 3.6	9.5	77.8 ± 2.6	1.2
25.5	86.3 ± 4.9	ND	ND	89.4 ± 1.1	3.1
154.7	100.0 ± 0.2	100.0	0.0	100.0	0

ND not detectable; $Y = \frac{HbO_2}{HbO_2 + Hb}$ (Hb saturation). $Y_{Optical}$ = Hb saturation determined by spectrophotometric measurement. Y_{Tyr-C7} = 100% − signal intensity of Tyr C7 = Hb saturation determined by NMR measurement of the Tyr C7 signal. $Y_{Val-E11}$ = Hb saturation determined by spectrophotometric measurement of the Val E11 signal, $\Delta_1 = (Y_{Optical} - Y_{Tyr-C7})$; $\Delta_2 = (Y_{Optical} - Y_{Val-E11})$; $PO_2 = (P_{Barometer} - P_{H_2O}) \times 0.209$. With IHP, optical experiment ($n = 3$); NMR experiment ($n = 7$). Without IHP, optical experiment ($n = 3$); NMR experiment ($n = 4$). Errors are expressed as standard deviation

10.98 to 17.05, consistent with the acid-Bohr effect. The Hill coefficient, however, shows no change. In the presence of IHP and pH 6.6, the P_{50} increases from 31.06 to 51.28 and n_{Hill} decreases from 2.52 to 2.29.

These Hb oxygen-binding curves agree with previous literature reports and validate the oxygen equilibration system's capacity to establish accurately the Hb saturation (Table 2; Ogata 2000; Vorger and Matelin 1985; Yonetani et al. 2002; Imai 1981). They also confirm the effectiveness of IHP, a stable analog of the endogenous allosteric effector BPG (2,3 bisphophoglycerate) in erythrocyte, to modulate the HbO$_2$-binding affinity and cooperativity. Without IHP or BPG, Hb exhibits a high O$_2$ affinity. Hb has a decreased efficiency in unloading O$_2$. With the allosteric effector IHP or BPG, Hb decreases its O$_2$ affinity. The O$_2$-binding curve shifts to the right (Levitzki 1978). Indeed, erythrocytes increase BPG level during physiological adaptation to high altitude in order to improve O$_2$ unloading in the capillary (Weber 2007).

Val E11 signal as a vascular PO_2 biomarker

The γCH$_3$Val E11 signal of Mb has presented an approach to measure the intracellular PO_2 in isolated myocardium

(Kreutzer et al. 1992). Since NMR studies have already observed the proximal histidyl $N_\delta H$ signals from erythrocyte, they implied the availability of the Val E11 and Tyr C7 signals as vascular PO_2 biomarkers in vivo (Kreutzer et al. 1993; Tran et al. 1999). Detecting the γCH_3 signal of Val E11 would immediately improve the detection sensitivity given the three-proton intensity of the CH_3 group versus one-proton intensity of the proximal histidyl $N_\delta H$. Moreover, it would overcome the requirement to secure a normalizing signal under anoxia, since the Val E11 signal reaches its maximal intensity under oxygenated conditions. However, its function as an oximeter must overcome the criticism that the Val E11 signal might not correspond to Hb saturation, since it does not have a direct role in propagating the quaternary structural perturbation as defined in the Perutz's interpretation of the Monod, Changeux and Wyman (MWC) two-state model of Hb oxygen binding (Fetler et al. 1995; Monod et al. 1965; Weissbluth 1974; Perutz 1989; Perutz et al. 1998; Bruno et al. 2001).

The present study shows that the Val E11 signal does track closely Hb saturation in the presence and absence of IHP and at different pH values. As Hb saturation increases or decreases, so also does the Val E11 signal intensity. Even though the Perutz model localizes the cooperativity energy in a specific set of quaternary structural changes, it does not dismiss the presence of tertiary structural changes during the R to T transition (Perutz et al. 1968; Muirhead et al. 1967). Such tertiary structural change can still reflect the Hb oxygenation state.

Tyr C7 signal as a vascular PO_2 biomarker

The correlation between the tertiary and quaternary structural changes becomes apparent in the comparative analysis of the Val E11 and Tyr C7 signals. From the NMR spectra, the Val E11 signal shows an inverse relation with the Tyr C7 signal, which originates from a T state sensitive hydrogen bond at the subunit interface. As Hb switches from the R to T state, the Perutz model specifies a hydrogen bond formation step (Ho and Russu 1981; Mihailescu and Russu 2001). In essence, the Tyr C7 peak at 14 ppm originating from a hydrogen bond at the $\alpha_1\beta_2$ subunit interface reports directly on the quaternary structure of Hb (Mihailescu and Russu 2001). This unique Hb signal provides an alternative to the proximal histidyl $N_\delta H$ signal of deoxy Mb to assess the deoxygenated state. As Hb desaturates and undergoes the R to T transition, the Tyr C7 signal increases correspondingly.

Both the Val E11 and Tyr C7 signals track closely the Hb saturation and imply that tertiary structural perturbation of Hb, even though unlinked with the direct control of O_2 affinity in the Perutz model, can still reflect the Hb saturation state. The observed correlation of both the Val E11

and Tyr C7 signals with the Hb saturation raises a question about imputing a specific localized structural change to explain fully the energetics of cooperativity (Shulman et al. 1975; Eaton et al. 1999).

Implications for in vivo vascular PO_2 measurements

Assessing the vascular PO_2 gradient in vivo poses many technical challenges. Yet, that measurement provides critical insight into the metabolic regulation in tissue. In the physiology field, many investigators have relied mainly on near infrared spectroscopy (NIRS) methods to assess the vascular PO_2 with the NIRS signal of Hb. Both oxygenated and deoxygenated Hb have absorbances at 760 and 850 nm. However, the deoxy Hb has a sharper and more intense absorbance than oxy Hb at 760 nm. The 760 and 850 nm absorption bands form then a basis to assess the overall tissue PO_2 (Jobsis 1977). Any blood volume change would affect both the oxy- and deoxy-Hb signals. By arguing that the NIRS signals originate predominantly from Hb, researchers have then presumed an exclusive measurement of the vascular PO_2 (Seiyama et al. 1988; Wilson et al. 1989; Seiyama et al. 1988). Unfortunately, Mb exhibits identical spectral features. Others have presented evidence to show that the NIRS signal contains a major Mb contribution (Hoofd et al. 2009; Nioka et al. 2009; Tran et al. 1999; Ponganis et al. 2008).

The ^1H NMR approach does not encounter the issue of overlapping spectra, for it can discriminate the Mb and Hb signals of the Val E11 and the proximal histidyl $N_\delta H$ (Kreutzer and Jue 1991; Kreutzer et al. 1992, 1993). Moreover, the Tyr C7 signal only appears in Hb. Even though some researchers have asserted that erythrocyte Hb signals do exhibit an NMR visible signal, many studies have presented experimental evidence countering such a viewpoint (Fetler et al. 1995; Ho and Russu 1981; Lindstrom and Koenig 1974; Wang et al. 1997). In fact, recent NMR experiments have detected the proximal histidyl $N_\delta H$ signal of deoxy Hb in human and seal skeletal muscle (Tran et al. 1999; Ponganis et al. 2008).

However, the algorithm to convert the Hb signals into vascular PO_2 differs from the process to obtain the intracellular PO_2 with the Mb signal. In the cell, the Mb content does not change. The proximal histidyl $N_\delta H$ or Val E11 peak intensity correlates directly with changes in the cellular PO_2. Blood volume, however, does not remain constant and can alter the signal intensity. Both blood volume and vascular oxygenation then can alter the signal intensity of Hb. Relying only on the normalized signal intensity of the deoxy Hb histidyl $N_\delta H$ or Val E11 will lead to an erroneous determination. Blood volume change, however, affects both the Val E11 and the proximal histidyl $N_\delta H$ signal. As a consequence, using the signal intensity ratio of Val E11 and proximal

histidyl $N_\delta H$ would overcome confounding contribution from blood volume and lead to the correct determination of the vascular PO_2 (Kreutzer et al. 1992).

Even though the present study has established the feasibility of using the Val E11 or Tyr C7 signal as a biomarker of the Hb oxygenation state, the implementation of a routine NMR method to determine vascular PO_2 in vivo still requires additional technical advances. These advances must address the interfering background signal arising from lipids and other endogenous molecules in the ^{1}H NMR spectra from typical 1.5 T scanners. Moreover, they must also provide some discrimination of the compartmentalized vascular PO_2 in arteries, veins and capillaries. Several studies have already begun to show some promising spectroscopic approaches (Lin et al. 2007). Nevertheless, the study has established that the Val E11 and Tyr C7 signals can report accurately the state of Hb oxygenation and will lead to new insights into the regulation of oxygen transport in tissue.

Conclusion

This study details an oxygen equilibration system that permits a comparative spectrophotometric and NMR determination of Hb saturation and which helps to address the utility of the Val E11 and the Tyr C7 as biomarkers of vascular PO_2. Under different PO_2, pH values and with or without IHP, the spectrophotometric assay of Hb saturation agrees with the NMR determination using the Val E11 and Tyr C7 signals. The oxygen-binding curves stand in excellent agreement with literature. Consequently, the results verify the validity of using either the Val E11 or Tyr C7 signals to assess Hb saturation and open a new direction to study vascular PO_2, oxygen transport and Hb structure–function.

References

Acharya SA, Malavalli A, Peterson E, Ho C, Manjula BN, Friedman JM (2003) Probing the conformation of hemoglobin presbyterian in the R-state. J Protein Chem 22:221–230

Antonini E, Brunori M (1971) Hemoglobin and myoglobin in their reactions with ligands. Elsevier, Amsterdam

Asakura T, Lau P (1978) Sequence of oxygen binding by hemoglobin. Proc Natl Acad Sci USA 75:5462–5465

Benesch R, Benesch RE, Yu CI (1967) Reciprocal binding of oxygen and diphosphoglycerate by human hemoglobin. Biochemistry 59:526–532

Bruno S, Bonaccio M, Bettati S, Rivetti C, Viappiani C, Abbruzzetti S, Mozzarelli A (2001) High and low oxygen affinity conformations of T state hemoglobin. Protein Sci 10:2401–2407

Chang CK, Simplaceanu V, Ho C (2002) Effects of amino acid substitutions at beta 131 on the structure and properties of hemoglobin: evidence for communication between alpha 1 beta 1- and alpha 1 beta 2-subunit interfaces. Biochemistry 41:5655

Chung Y, Mole PA, Sailasuta N, Tran TK, Hurd R, Jue T (2005) Control of respiration and bioenergetics during muscle contraction. Am J Physiol Cell Physiol 288:C730–C738

Dalvitt C, Ho C (1985) Proton nuclear overhauser effect investigation of the heme pockets in ligated forms hemoglobin conformational differences between oxy and carbonmonoxy form. Biochemistry 24:3398–3407

Eaton WA, Henry ER, Hofrichter J, Mozzarelli A (1999) Is cooperativity oxygen binding by hemoglobin really understood? Nature Struct Biol 6:351–358

Fetler BK, Simplaceanu V, Ho C (1995) ^{1}H NMR investigation of the oxygenation of hemoglobin in intact human red blood cells. Biophys J 68:681–693

Gong Q, Simplaceanu V, Lukin JA, Giovannelli JL, Ho NT, Ho C (2006) Quaternary structure of carbonmonoxyhemoglobins in solution: structural changes induced by the allosteric effector inositol hexaphosphate. Biochemistry 45:5140–5148

Ho C, Russu I (1981), Proton nuclear magnetic resonance investigation of hemoglobins. Methods in Enzymology, Academic, New York

Hoofd L, Colier W, Oeseburg B (2009) A modeling investigation to the possible role of myoglobin in human muscle in near infrared spectroscopy (NIRS) measurements. Adv Exp Med Biol 530:637–643

Hore PJ (1983) A new method for water suppression in the proton NMR spectra of aqueous solutions. J Magn Reson 54:539–542

Imai K (1981) Measurement of accurate oxygen equilibrium curves by an automatic oxygenation apparatus. Methods Enzymol 76:438–449

Jobsis FF (1977) Noninvasive, infrared monitoring of cerebral and myocardial oxygen sufficiency and circulatory parameters. Science 198:1264–1267

Jue T (1994) Measuring tissue oxygenation with the ^{1}H NMR signals of myoglobin. In: Gillies RJ (ed) NMR in physiology and biomedicine. Academic Press, New York

Kreutzer U, Jue T (1991) ^{1}H nuclear magnetic resonance deoxymyoglobin signal as indicator of intracellular oxygenation in myocardium. Am J Physiol 30:H2091–H2097

Kreutzer U, Wang DS, Jue T (1992) Observing the ^{1}H NMR signal of the myoglobin Val-E11 in myocardium: an index of cellular oxygenation. Proc Natl Acad Sci USA 89:4731–4733

Kreutzer U, Chung Y, Butler D, Jue T (1993) ^{1}H-NMR characterization of the human myocardium myoglobin and erythrocyte hemoglobin signals. Biochim Biophys Acta 1161:33–37

Levitzki A (1978) Quantitative aspects of allosteric mechanism. Springer, Berlin

Lin PC, Kreutzer U, Jue T (2007) Anisotropy and temperature dependence of myoglobin translational diffusion in myocardium: implication on oxygen transport and cellular architecture. Biophys J 92:2608–2620

Lindstrom TR, Koenig SH (1974) Magnetic field-dependent water proton spin lattice relaxation rates of hemoglobin solutions and whole blood. J Magn Reson 15:344–353

Lukin JA, Ho C (2004) The structure–function relationship of hemoglobin in solution at atomic resolution. Chem Rev 104:1219–1230

Mihailescu MR, Russu IM (2001) A signature of the T $\rightarrow$ R transition in human hemoglobin. Proc Natl Acad Sci USA 98:3773–3777

Monod J, Wyman J, Changeux JP (1965) On the nature of allosteric transitions: a plausible model. J Mol Biol 8:8–118

Muirhead H, Cox JM, Mazzarella L, Perutz MF (1967) Structure and function of haemoglobin. 3. A three-dimensional Fourier synthesis of human deoxyhaemoglobin at 5.5 Angstrom resolution. J Mol Biol 28:117–156

Nioka S, Wang DJ, Im J, Hamaoka T, Wang ZJ, Leigh JS, Chance B (2009) Simulation of Mb/Hb in NIRS and oxygen gradient in the human and canine skeletal muscle using H-NMR and NIRS. Adv Exp Med Biol 578:223–228

Ogata Y (2000) Characteristics and function of human hemoglobin vesicles as an oxygen carrier. Polym Adv Technol 11:205–209

Perutz MF (1989) Mechanisms of cooperativity and allosteric regulation in proteins. Q Rev Biophys 22:139–236

Perutz MF, Muirhead H, Cox JM, Goaman LC (1968) Three-dimensional Fourier synthesis of horse oxyhaemoglobin at 2.8 A resolution: the atomic model. Nature 219:131–139

Perutz MF, Wilkinson AJ, Paoli M, Dodson GG (1998) The stereochemical mechanism of the cooperative effects in hemoglobin revisited. Annu Rev Biophys Biomol Struct 27:1–34

Ponganis PJ, Kreutzer U, Stockard TK, Lin PC, Sailasuta N, Tran TK, Hurd R, Jue T (2008) Blood flow and metabolic regulation in seal muscle during apnea. J Exp Biol 211:3323–3332

Rossi-Fanelli A, Antonini E, Caputo A (1961) Studies on the relations between molecular and functional properties of hemoglobin. II. The effect of salts on the oxygen equilibrium of human hemoglobin. J Biol Chem 236:397–400

Seiyama A, Hazeki O, Tamura M (1988) Noninvasive quantitative analysis of blood oxygenation in the rat skeletal muscle. J Biochem 103:419–424

Shulman R, Hopfield JJ, Ogawa S (1975) Allosteric interpretation of hemoglobin properties. Q Rev Biophys 8:325–420

Tran TK, Sailasuta N, Kreutzer U, Hurd R, Chung Y, Mole P, Kuno S, Jue T (1999) Comparative analysis of NMR and NIRS measurements of intracellular PO_2 in human skeletal muscle. Am J Physiol 276:R1682–R1690

Viggiano G, Ho C (1979) Proton nuclear magnetic resonance investigation of structural changes associated with cooperative oxygenation of human adult hemoglobin. Proc Natl Acad Sci USA 76:3673–3677

Viggiano G, Ho NT, Ho C (1979) Proton nuclear magnetic resonance and biochemical studies of oxygenation of human hemoglobin in deuterium oxide. Biochemistry 18:5238–5247

Vorger P, Matelin D (1985) A low cost apparatus for the automatic determination of precise oxygen equilibrium curves on red blood cell suspensions. Comp Biochem Physiol 82:355–359

Wang D, Kreutzer U, Chung Y, Jue T (1997) Myoglobin and hemoglobin rotational diffusion in the cell. Biophys J 73:2764–2770

Weber RE (2007) High-altitude adaptations in vertebrate hemoglobins. Respir Physiol Neurobiol 158:132–142

Weissbluth M (1974) Cooperativity and electronic properties. Mol Biol Biochem Biophys 15:1–175

Wilson JR, Mancini DM, McCully K, Feraro N, Lanoce V, Chance B (1989) Noninvasive detection of skeletal muscle underperfusion with near-infrared spectroscopy in patients with heart failure. Circulation 80:1668–1674

Yonetani T, Park SI, Tsuneshige A, Imai K, Kanaori K (2002) Global allostery model of hemoglobin. Modulation of O(2) affinity, cooperativity, and Bohr effect by heterotrophic allosteric effectors. J Biol Chem 277:34508–34520